NASA Technical Paper 1098

Hydrogen Film Cooling of a Small Hydrogen-Oxygen Thrust Chamber and Its Effect on Erosion Rates of Various Ablative Materials

Ned Hannum, William E. Roberts, and Louis M. Russell

DECEMBER 1977

NASA

NASA Technical Paper 1098

Hydrogen Film Cooling of a Small Hydrogen-Oxygen Thrust Chamber and Its Effect on Erosion Rates of Various Ablative Materials

Ned Hannum, William E. Roberts,
and Louis M. Russell

Lewis Research Center
Cleveland, Ohio

National Aeronautics
and Space Administration

**Scientific and Technical
Information Office**

1977

HYDROGEN FILM COOLING OF A SMALL HYDROGEN-OXYGEN THRUST CHAMBER AND ITS EFFECT ON EROSION RATES OF VARIOUS ABLATIVE MATERIALS

by Ned Hannum, William E. Roberts, and Louis M. Russell

Lewis Research Center

SUMMARY

An experimental investigation was conducted to determine what arrangement of film-coolant-injection holes could be used to decrease the erosion rates in small, high-temperature, high-pressure ablative thrust chambers without incurring large penalties in combustion performance. The effect of the selected film-coolant arrangement on the erosion rates of 19 ablative materials was then determined. Film cooling was applied to reduce the wall temperature and ablative erosion at high combustion temperatures and pressures.

All of the film cooling arrangements tested were symmetrically placed axial holes or groups of holes located on a ring between the outer row of injector elements and the chamber wall. The best arrangement, which had twice the number of holes as there were elements in the outer row, was also the simplest. The performance penalty for this type of cooling, presented as a reduction in characteristic exhaust velocity efficiency, was 0.8 percentage point when 10 percent of the total hydrogen (fuel) flowed through the coolant holes and 2.8 percentage points when 20 percent of the fuel flow was used as coolant. The throat erosion rate was reduced by a factor of 2.5 when 10 percent of the fuel flow was used as coolant.

Nineteen ablative materials were tested using the best film-coolant injector design. Even with film cooling, only the more expensive silica-phenolic ablative materials had low enough erosion rates to be considered for use as throat materials for rocket engines whose chamber pressures reach 3450 kilopascals (500 psia). Some of the cheaper materials might qualify for use in other areas of the nozzle where heat flux is low or for use in large throat diameter nozzles where higher erosion rates are acceptable.

INTRODUCTION

Ablative materials have been used extensively in liquid-propellant rocket thrust chambers where pressures are usually 690 kilopascals (100 psia) or less. In general, only silica-phenolic materials have been capable of providing acceptable throat erosion rates. The present study investigates the use of less expensive ablative materials to line work horse combustion chambers. These chambers are used for injector check-outs, combustion investigations, powerhead studies, etc.

The specific objective of this program was to create a more benign environment for the combustor walls by establishing a low temperature, low-mixture-ratio region near the wall with the hope that a relatively inexpensive ablative combustor might be used satisfactorily even at chamber pressures up to 3450 kilopascals (500 psia). The injector element sizes and combustor lengths chosen were typical of large diameter engines. Significant cost savings on ablatives for small engines is difficult, but with large, booster engines there is an opportunity to effect big savings.

Baseline tests were conducted to (1) document the performance of the injector and (2) determine gouge locations on and erosion rates of the combustor walls with standard ablative materials when no film cooling was used. Various arrangements of fuel-film-cooling orifices were then evaluated. Each configuration was evaluated for its (1) effect on combustion performance, (2) effect on circumferentially irregular erosion or gouging, and (3) overall effect of reducing the wall temperature as indicated by a reduction in average erosion rate.

To reduce the cost of the fuel-film-cooling development and to accelerate the screening of the fuel-film-cooling configurations, much of the testing was conducted with chambers fabricated from an indicator material instead of the more expensive ablatives. The material chosen was unreinforced phenolic or Bakelite which was shown to erode much like the ablative materials except at a higher rate.

Nineteen ablative materials were tested using the best fuel-film-cooling configuration. The materials included possible throat materials as well as materials for use in much lower heat flux, shear, or temperature regions, but in all cases the materials were tested as convergent-divergent nozzle sections.

APPARATUS

Test Facility

The investigation was conducted in the rocket engine test facility at the Lewis Research Center. This is a 223-newton (50 000-lbf) thrust sea-level rocket test stand

equipped with an exhaust gas muffler and scrubber. The rocket engines were mounted on a thrust stand to fire vertically downward into the scrubber. The facility used a pressurized propellant system to deliver the propellants to the engine from the storage tanks. The oxygen propellant line and storage tank were immersed in a liquid-nitrogen bath. The liquid-hydrogen line was vacuum-jacketed and insulated with foam.

Thrust-Chamber Assembly

The rocket thrust-chamber assembly comprised a concentric tube injector, a 14.27-centimeter (5.62-in.) inside-diameter cylindrical chamber, and a convergent-divergent exhaust nozzle with a contraction ratio of 1.9 and an expansion ratio of 1.3. The thrust chamber was 74 centimeters (29 in.) from injector face to throat.

Injector

The injector comprised 37 concentric tube elements. A cross section of an injection element is shown in figure 1, and a faceplate view showing the arrangement of the elements is shown in figure 2. The fuel film cooling was accomplished by introducing extra hydrogen between the outer row of elements and the combustor wall. For ease of modification the film-cooling holes were located in a ring (fig. 2) that fit into the area between the outer row of elements and the combustor wall. Two film-cooling schemes were used: (1) hydrogen-coolant streams parallel to the injector element axis, and (2) hydrogen-coolant streams impinging on the propellant streams. The description and dimensions of each film-cooling scheme are given in figure 3. The impingement distances were either 1.27 or 3.81 centimeters (0.5 or 1.5 in.) from the injector face. The nominal amount of coolant flow was either 10 or 20 percent of the total hydrogen flow.

Chamber

Four chamber-nozzle combinations were used in the investigation: (1) a heat-sink chamber fabricated from zirconium oxide coated steel was combined with a graphite nozzle for use in determining the performance characteristics of the injector; (2) chambers, made by stacking 2.54-centimeter (1-in.) thick Bakelite rings, were run with graphite nozzles to evaluate the film-cooling configurations (fig. 4); (3) one-piece thrust chambers, made from a silica-phenolic ablative material, were used to establish the

baseline erosion characteristics in the combustion chamber with no fuel film cooling; and (4) cylindrical chambers made of silica-phenolic ablative material (no. 5) were used for the materials investigation of the 19 nozzles listed in table I. (See also fig. 5.)

Instrumentation and Flow Measurement

The location of the various transducers and the associated flow lines is shown by the schematic diagram of figure 6.

The liquid-oxygen flow rate was measured with a water calibrated turbine flowmeter. The liquid-hydrogen flow rate was measured by a venturi (also water calibrated) submerged in the supply tank. The calibration for each of these cryogenic flow-measuring instruments was corrected for dimensional changes from the ambient temperature water calibrations.

Since the film coolant and the main fuel were at the same temperature, the fuel flow rate through the film-coolant holes was assumed to be proportional to the area divided by the total fuel-injection area. This was possible because the differential pressures across both the film-coolant orifices and the main injection-element annuli were equal. This flow split fraction is shown in figure 3 as the ratio of zone area to total area. The flow characteristics distribution of each film-cooling configuration was confirmed by water flow tests. An annular Plexiglass catch tank was fabricated and divided into 18 compartments corresponding to the 18 injection elements in the outer row of the injector. Each film-cooling ring was then water flowed over this catch tank for a measured amount of time with care taken to account for dribble volumes. From these tests each coolant hole or set of coolant holes was deburred by hand until all sets flowed nearly equal volumes in equal time.

Pressure and Temperature Measurement

Steady-state pressure measurements were made with strain-gage-element transducers. Bench calibrations were made before transducers were installed, and periodic in-place calibrations were performed by pressurizing the engine with nitrogen gas. The liquid propellant temperatures were measured with platinum resistance thermometers. All pressure and temperature transducers were electrically calibrated immediately before data acquisition by an electrical, two-step calibration system that used shunt resistances in a bridge circuit to simulate given conditions.

Data Acquisition

Signals from the transducers were transmitted to the control room and to an automatic digital data recording system. Oscillographs were used to obtain preliminary data between firings. The primary data were recorded with the digital system using a 6.25-kilohertz sweep rate over a block of 125 channels of information, thus providing a set of data every 0.02 second.

PROCEDURE

Engine Operation and Control

Before each firing the propellant tanks were pressurized with helium gas. All valves were sequenced with a solid-state timer. Individual automatic closed-loop controllers were used to maintain a constant chamber pressure and oxidant-fuel mixture ratio. The run duration was also controlled by a solid-state timer. An automatic cutoff, which monitored propellant flow rate, was used to terminate any firings when the throat area increase exceeded 25 percent. Automatic or manual shutdowns could be made when vital parameters exceeded acceptable limits or if leaks or fires were observed in the test cell.

Throat and Chamber Measurements

New ablative throat diameters were measured with a micrometer. After a firing and erosion or surface roughening had occurred, the throats, mounted in a machinists indexing attachment, were measured enough times to characterize the posttest condition. This method was used to determine erosion at stations through both the converging and diverging sections of the nozzles. The relative gouging characteristics of each fuel-film-cooling configuration were determined by placing individual Bakelite rings on polar graph paper, tracing the inner contour, then reading directly from the plot the erosion at precise circumferential locations. The plots were also planimetered to determine an area which in turn was used to determine a radius of a circle of equivalent area. From these data, an average chamber erosion was determined. Chamber erosion rates were calculated by dividing the average erosion by the total firing time. It is estimated that the erosion rates shown are accurate to within ±15 percent. The units for reporting erosion rate are millimeters per second (mil/sec).

The average chamber erosion with an ablative chamber was determined by averaging several diameter measurements, all made in the same plane, then reporting the average change in radius divided by the total firing time as erosion rate.

Radius changes in the throat plane were determined as a function of firing time using the method described in reference 1. This method assumes constant characteristic exhaust velocity efficiency and assumes that any changes in either chamber pressure or total propellant flow rate are related to changes in the area of the throat.

RESULTS AND DISCUSSION

The selection of the best film-coolant arrangement will be presented and discussed first. Included in this discussion will be the effect of fuel film cooling on combustion performance and the improvement in erosion characteristics with the standard silica-phenolic ablative material (no. 5 of table I). Next, erosion data for the 19 different ablative materials used in conjunction with the best fuel-film-cooling scheme will be presented.

An example of test results with an indicator material is shown in figure 7. The average erosion rates in the cylindrical portion of the long combustion chamber at a station 61 centimeters (24 in.) from the injector are compared for both the Bakelite indicator material and the standard silica-phenolic ablative material. These materials have similar trends of increasing erosion rate with increasing mixture ratio and, therefore, it was concluded that the Bakelite was a good indicator material. The Bakelite erosion rate is approximately seven times greater than the ablative. When no fuel film cooling was used, the gouge pattern in the chamber was similar for both materials. The gouges mirrored the outer row of 18 coaxial injection elements. At higher oxidant-fuel ratios, the gouges were deeper and persisted farther down the wall than at low oxidant-fuel ratios.

To eliminate the gouging effect and to reduce the average erosion rate, several configurations of film-coolant holes were tried with two film-coolant flow rates. In four the coolant streams impinged the outer-row injection streams; in the other three the coolant streams were parallel to the wall.

Selection of Fuel-Film-Cooling Configuration

The following erosion rate data are for Bakelite lined chambers. As you can see in figure 8, the data plot reasonably well as straight lines when log-log coordinates are used. The effect of oxidant-fuel mixture ratio O/F on chamber erosion rate when no

fuel film cooling was used is shown in figure 8(a). At O/F = 4.7 the chamber wall erosion was about $1\frac{1}{2}$ to 2 times greater than that at O/F = 3.2. At the higher O/F the erosion rate was fairly constant all the way down the chamber; at the lower O/F the erosion rate tended to increase gradually with increasing distance from the injection plane.

Also shown in figure 8(a) is the effect of two fuel-film-cooling flow rates on erosion. When compared with erosion rate with no film cooling, at about the same overall oxidant fuel ratio, a 10-percent hydrogen (coolant) flow through parallel stream configuration 1B reduced chamber erosion rate threefold 15 centimeters (6 in.) from the injector face, and a 20-percent coolant flow through a similar configuration 1A reduced the erosion rate twelvefold at the same distance from the injector face. Downstream of this location the erosion rate reductions grew progressively smaller. In fact, at 61 centimeters from the injector face, the erosion rotor for configurations 1B and 1A were the same, but they were still 2/3 of the rate without film cooling.

A comparison of the two sets of data in figure 8(a) reveals the significant reduction in erosion rate over the entire length of the chamber that occurs when fuel film cooling is used. Note also that, although 20 percent coolant flow is much better than 10 percent coolant flow near the injector, it is no better 61 centimeters (24 in.) from the injector.

The effect on chamber erosion rate of impinging the fuel film cooling on the outer-row injector element streams is shown in figure 8(b). At an overall O/F of 4.0 and with 20 percent coolant flow, there was no major difference in the erosion rates of impinging stream configurations 3 to 5 at any axial station. There was a concern that the effectiveness of the impinging configurations would be drastically reduced if there was a misalinement of the film-cooling streams and the oxygen propellant injection streams. Consequently, configuration 4 was rotated 3° and tested. The erosion rate near the injector face increased appreciably at the same O/F and coolant flow, which confirmed the importance of alinement. (The erosion rates nearer the throat were not changed.)

The data of figure 8(c) at an overall O/F of 4.8 and with a 10-percent coolant flow show that an impinging stream configuration (6) was less effective in preventing chamber erosion than a parallel stream configuration 1B.

The effect of hole spacing is shown in figure 8(d). The data show that, at an overall O/F of 4.9 and with 20 percent parallel coolant flow, 36 equally spaced streams (configuration 1A) were more effective in preventing chamber erosion than 36 streams composed of 18 pairs, each pair 0.5 centimeter (0.2 in.) apart (configuration 2).

Another concern in using film cooling is the loss of combustion performance. The experimental characteristic exhaust velocities C* of configuration 1 and of the no-film cooling case are shown in figure 9 as functions of oxidant-fuel ratio. The experimental characteristic exhaust velocity data are presented with an estimated precision of ±0.3 percent for one standard deviation. In figure 9(a) the C* data for the no-film cooling case are presented. By comparing the experimental data with the theoretical equilib-

rium composition data, it can be seen that between O/F's of 4 and 6 the performance is constant at approximately 99.3 percent but that at an O/F of 3, the performance is reduced to 98.4 percent of theoretical C*. When film cooling is added, the performance curve is shifted to the left because of the imposed maldistribution of the hydrogen. This is shown in figure 9(b) for both 10 and 20 percent coolant flows (configurations 1B and 1A). The result is that, at an O/F of 5, the addition of film cooling reduces the performance to 98.5 percent with 10 percent coolant flow and to approximately 96.5 percent with 20 percent coolant flow. (The comparison with 20 % coolant flow requires some extrapolation of the data.) However, at an O/F of 3 the use of 10 percent coolant flow actually increases performance by approximately 1 percent above the no-film cooling case, and the use of 20 percent coolant flow produces about the same performance as the no-film cooling case. (Combustion performance was measured for configurations 1A and 1B only.) Similar effects on performance when using mixture ratio zoning in rocket combustors have been reported (ref. 1) using nitrogen tetroxide and a blend of 50 percent hydrazine and 50 percent unsymmetrical dimethyl hydrazine as propellants.

In summary, the selction of the film-cooling configuration to be used in the materials testing was made by considering the erosion data and the combustion performance data. Chamber erosion rate near the throat (61 cm (21 in.)) was about the same for both 10 and 20 percent coolant flows (figs. 8(a)). Therefore, because of its higher performance, a 10-percent film-cooling configuration was selected. From a fabrication standpoint the parallel configurations are preferred over the impinging stream configurations. Further support for choosing the simpler configuration results from these facts: Parallel and impinging configurations provide nearly equal erosion rates near the throat (see fig. 8(c)), and the combustion performance of configuration 1B was quite acceptable (fig. 9). Therefore, configuration 1B was selected for use in the materials testing. It should be noted that the selection of configuration 1B was made from comparison of test results using Bakelite chambers and did not include erosion data in the throat plane. To establish the quantitative effects of using configuration 1B, tests were conducted using fully ablative lined chambers and nozzles assembled as shown in figure 5. The nozzle sections were made from silica-phenolic material 2. (See table I.) The cylinder chambers were lined with silica-phenolic 5. The 20-second tests were made at constant O/F and chamber pressure (3450 kPa (500 psia)) using the automatic control described in the PROCEDURE section. The average throat erosion rates with configuration 1B and without film cooling are shown in figure 10 as functions of mixture ratio. The data for an O/F of 5 show that the use of 10 percent coolant flow reduced the erosion rate at the throat from 0.26 to 0.1 millimeter per second (10.2 to 4.0 mil/sec). During a 20-second test using 10-percent coolant flow at an O/F of 3.9, there was no throat erosion.

Although the present data were taken using a small thrust chamber (diam, 14.27 cm (5.62 in.)), some discussion about the use of film cooling in larger diameter engines is appropriate. During the development program for the 6.68×10^6-newton (1.5×10^6-lbf) thrust M-1 injector, ablative materials were used for the combustion chambers, and tests were conducted at chamber pressures of 3930 and 7170 kilopascals (570 and 1040 psia). The materials used were a silica-phenolic quite similar to material 2 of this report. The measured average erosion rates during tests with the M-1 chambers at a chamber pressure of 3930 kilopascals (570 psia) were very close to those presented for material 2. For the M-1 tests, 3.7 percent of the total hydrogen flow was introduced as film coolant. The M-1 thrust chamber is 107 centimeters (42 in.) in diameter. For the same ablative erosion rate, the percentage of hydrogen flow needed for film cooling decreases with increasing chamber diameter. Consequently, the performance penalty of using film cooling in large-diameter chambers should also decrease.

Ablative Material Evaluation

The testing of the 19 materials was done in a test chamber like that shown in figure 5. The test piece in each case was the nozzle section only. For each test, a new cylindrical liner made from material 5 (table I) was used. Film-cooling configuration 1B was used in all tests.

The nominal chamber pressure was 3450 kilopascals (500 psia). The mixture ratio (including the coolant) selected for the material evaluation was 4.5. This mixture ratio was a compromise between the higher O/F often preferred in the vehicle design and the lower O/F preferred when using ablative liners. Each test lasted 20 seconds unless there was a 25-percent change in throat area before that time (as indicated by 25 % increase in oxidizer flow rate), in which event the test was terminated.

Throat erosion data for the 19 ablative materials are shown in figure 11. The test materials are described in table I. The lowest throat erosion rates were obtained with the six silica-phenolic materials (group A of fig. 11). These materials are generally the most expensive. The next best group of materials (group B of fig. 11) consisted of silica-aluminum phosphate and silica-phenolic carborazole. These materials eroded 3 to 4 times faster than the first group. A single silica-rubber material (group C of fig. 11) produced an erosion rate 7 or 8 times greater than the silica-phenolic group. Asbestos-phenolics and glass-phenolics were in the next group (group D of fig. 11) of materials. The fastest eroding group of materials (group E of fig. 11) included silica-polyurethane; silica, asbestos-acrylic rubber; glass polyvinylchloride (PVC); silica, asbestos-rubber; and asbestos-PVC.

Silica was the most used reinforcement material. The form and orientation of the silica used as reinforcement was not an independent variable in the materials selected for testing. Consequently, the preferred method of using silica was not determined. Consideration must be given to the cost of fabrication and to the ease of repair as noted in table I.

The authors of reference 1 report that the throat erosion rate with silica-phenolic ablative materials correlates very well with temperature. Usually the temperature used for correlation is the theoretical combustion gas temperature. But because filming cooling was being used in the M-1 testing, the erosion rate data of reference 2 are plotted as a function of an empirically derived wall temperature and for a chamber pressure of 3930 kilopascals (570 psia). A curve, which has been faired through the reference 2 data, is presented in figure 12(a). For wall temperatures less than 1722 K (3100° R) erosion rate was less than 0.01 millimeter per second (0.4 mil/sec). However, as wall temperature increased further, there was a rapid increase in erosion rate. As an example, at 2278 K (4100° R) the erosion rate was 0.25 millimeter per second (10 mil/sec). No data are reported for wall temperatures above this value. It should be noted that silica begins to soften at approximately 1778 K (3200° R) and will completely melt at approximately 2166 K (3900° R). From these data it would seem that the throat erosion rate is temperature related up to the complete melt temperature of the silica. Above that temperature, other factors, such as shear forces, probably control the erosion rate, which is likely to be very high.

The throat erosion rate data of reference 1 are shown in figure 12(b) as a function of combustion gas temperature instead of wall temperature. Also shown in that figure are data from the present testing. Because the data from reference 1 were taken using nitrogen tetroxide and a blend of 50 percent hydrazine and 50 percent unsymmetrical dimethyl hydrazine at a chamber pressure of 690 kilopascals (100 psia), the temperatures are lower than with the present data using hydrogen and oxygen at a chamber pressure of 3450 kilopascals (500 psia). Still, all the data plot along the same straight line. The erosion data presented in figure 12(b) are for nozzles with small throat diameters, whereas the data presented in figure 12(a) are for large throat diameter nozzles, where, it is postulated, similar conditions should produce lower erosion rates. Also, as previously mentioned, the correlating temperatures are different, that is, wall temperature in figure 12(a) and combustor gas temperature in figure 12(b). Although a direct overlay of these two figures cannot be made, it is believed that, because the erosion rate data of figure 12(b) increases gradually with increasing combustion gas temperature, the wall temperature for the data must be below the complete melt temperature of the silica and therefore corresponds to the flatter part of the curve in figure 12(a). For the data of this report and that of reference 1, it appears that the wall temperature (1) was the primary control of the erosion rate and (2) was less than the com-

plete melt temperature of silica (i.e., 2166 K (3900° R).

From the previous results it is obvious that many of these materials could not be considered as candidate throat materials for this diameter throat and chamber pressure. However, these materials may be suitable for lower heat flux, lower temperature, or lower shear environments.

Local erosion rate data for material 4(silica-phenolic materials from group A) and for material 18 (silica-phenolic-carborazole from group B) are presented in figure 13 as a function of Mach number. The Mach number was computed assuming isentropic flow and was therefore only a function of nozzle area ratio and a nominal value of the ratio of specific heat of the combustion products. Because the erosion rate is related to heat flux, temperature, and shear forces and because Mach number enters into the determination of each of these, it was chosen as a correlating parameter. For reference, the analytically computed heat flux for this engine at Mach numbers of 0.33, 1.0, and 1.75 was nominally 14.7, 26.3, and 6.5 megawatts per square meter per second (9, 16, and 4 Btu/in^2 · sec), respectively.

The erosion rates shown in figure 13 were determined by taking radius measurements at precisely located axial stations along the nozzle. The shape of the plot is typical for all of the materials. Erosion rate data for all the materials are tabulated in table II for Mach 0.33 and 1.75 and at the peak value, which occurs between Mach 0.8 to 1.2.

The selection of ablative materials for use in rocket combustion chambers and nozzles requires the consideration of cost, erosion rate requirements, and the ease of fabrication and repair. The approximate cost per pound in large lots is tabulated in table II for the better materials. The other materials have not been produced in large lots and consequently, cost information is not available. When low erosion rates and run lengths of several seconds are required, only the more expensive silica-phenolic materials can be considered for use in the throat plane of small-diameter, 3450-kilopascal (500-psia) rocket chambers. Some of the lower-cost - higher-erosion-rate materials might be usable if the percentage of film coolant is increased. Increasing the percentage of film coolant could be done in large-diameter combustors without serious loss in combustion performance. Substantial cost savings do appear possible by using silica-aluminum phosphate at Mach numbers other than 1, especially in large-diameter chambers. Also, because of the trend of lower erosion rate at low O/F, a cost saving may be accomplished by reducing the combustion chamber O/F. Other considerations in selecting a material may be the fabrication or repair process, that is, trowelable, castable, ribbon wrap over a mandrel, sheets wrapped over a mandrel, or sheets die cut and bonded into a stack. Table I notes some of these characteristics for the materials tested.

SUMMARY OF RESULTS

During a test program to investigate the use of fuel film cooling in conjunction with ablative lined thrust chambers and nozzles, 6 different film cooling configurations were evaluated and 19 different ablative materials were tested. The chamber pressure was 3450 kilopascals (500 psia) and the oxidant-fuel ratio for the liquid oxygen and liquid hydrogen propellants was from 3 to 6. Film cooling using 10 and 20 percent of the fuel were evaluated. The following results were obtained:

Selection of Fuel-Film-Cooling Scheme

1. Large reductions in both average chamber and average throat erosion rates were obtained in ablative engines with lengths of 74 centimeters (29 in.) to the throat by using fuel-film cooling.

2. For a small throat diameter (9.93 cm (3.91 in.)) engine operating at a chamber pressure of 3450 kilopascal (500 psia) and an oxidant-fuel mixture ratio of 4.8, 10 percent of the fuel flow used as film coolant reduced the erosion rate of Bakelite by a factor of 3 at 15 centimeters from the injector and by a factor of 1.5 at 61 centimeters from the injector. Using 10 percent fuel film cooling with silica-phenolic ablative reduced the throat erosion rate (74 cm (29 in.) from the injector) by a factor of 2.5.

3. Also, for a small throat diameter engine, using 10 percent fuel film cooling reduced the characteristic exhaust velocity C* 0.8 percentage points, and using 20 percent fuel film cooling reduced the C* 2.8 percentage points at a mixture ratio of 5.0.

4. The most effective and least complicated fuel-film-coolant scheme was to apply the coolant in parallel streams located symmetrically around the circumference of the engine with one hole opposite each outer-row injection element and one hole between two injection elements.

Selection of Appropriate Ablative Materials

5. For throat applications (Mach 1) where test firings are to be several seconds long, only the more expensive silica-phenolic materials had low erosion rates.

6. Silica-aluminum phosphate or silica-phenolic carborazole may be used at Mach numbers less than 0.33 or greater than 1.75.

7. The erosion rate at a chamber pressure of 3450 kilopascals (500 psia) may be greatly reduced by reducing the combustion chamber mixture ratio. One silica-phenolic

material produced a zero erosion rate at an oxidant-fuel mixture ratio of 3.9 after a 20-second firing.

Lewis Research Center,
National Aeronautics and Space Administration,
Cleveland, Ohio, August 12, 1977,
506-21.

REFERENCES

1. Winter, Jerry M.; Pavli, Albert J.; and Shinn, Arthur M., Jr.: Design and Evaluation of an Oxidant-Fuel-Ratio-Zoned Rocket Injector for High Performance and Ablative Engine Compatibility. NASA TN D-6918, 1972.

2. Kovach, R. J.; Mellish, J. A.; and Michel, R. W.: Large Hydrogen-Oxygen Ablative Chamber Test Program. (AGC-9400-15, Aerojet-General Corp.; NAS3-11214) NASA CR-72512, 1969.

TABLE I. - NOZZLE MATERIALS EVALUATED

Material number	Binder		Additive		Reinforcement			Orientation	Normalized cost per unit weight, $	Reason for selection
	Type	wt %	Type	wt %	Material	Form	wt %			
1	Phenolic	39	----------	----	Silica	Cloth	61	90° center-line	6	Effect of removing SiO_2 powder
2	Phenolic	20 - 25	----------	----	Silica	Cloth	75 - 80	90° center-line	8	Effect of maximizing reinforcement
3	Phenolic polyamide	27	----------	----	Silica chrome salt	Cloth	73	90° center-line	10	Effect of melt viscosity
4	Phenolic	27	----------	----	Silica	1.27- by 1.27-cm squares	73	Random	9	Effect of high viscosity and chopped reinforcement
5	Phenolic	31	ZrO_2 powder	----	Silica	Cloth	61	90° center-line	6	ZrO_2 filler effect
6	↓	40	----------	----	Asbestos	Fiber	60	Random	3	Low cost
7		30	----------	----	Asbestos	Fiber	70	Random	4	Effect of adding reinforcement
8		40	----------	----	Glass	Cloth	60	90° center-line	2	Low cost
9		↓	----------	----	Glass	Chopped roving	↓	Random	1	Trowelable, low cost
10			----------	----	Asbestos	Chopped yarn		↓	2	Trowelable, low cost
11			----------	----	Silica	Chopped roving			3	Trowelable, low cost
12	Aluminum phosphate	30	Al_2O_3	10	Silica	1.27- by 1.27-cm squares			1	Castable, low cost
13	Polyvinyl-chloride	40	----------	----	Asbestos	Fiber			2	Low cost
14	Polyvinyl-chloride	40	----------	----	Glass	Fiber	↓		1	Low cost
15	Rubber	----	----------	----	Silica asbestos	Fiber	----		----	Sheet application
16	Rubber	----	----------	----	Silica	Fiber	----	↓	----	Castable or trowelable
17	Acrylonitrile-butadiene	----	----------	----	Silica asbestos	----------	----	----------	----	----------
18	Phenolic carborazole	----	----------	----	Silica	----------	----	----------	----	----------
19	Poly-urethane	----	----------	----	Silica	----------	----	----------	----	Castable

TABLE II. - COMPARISONS OF EROSION RATE AND COST FOR TWO MACH NUMBER APPLICATIONS

Material			Normalized cost per unit weight, $	Mach number					
				0.33		1.75		Peak value[b]	
				Erosion rate					
Group	Name	Number[a]		mm/sec	mil/sec	mm/sec	mil/sec	mm/sec	mil/sec
A	Silica-phenolic	1	6	0	0	0	0	0.10	4.0
		3	10	.13	.5	.13	.5	.01	.5
		2	8	0	0	.05	.2	.06	2.3
		11	3	.10	.4	0	0	.23	9.1
		4	9	.03	.1	0	0	.10	3.8
		5	6	.17	.65	0	0	.14	5.7
B	Silica-aluminum phosphate	12	1	0.13	0.5	0	0	0.23	9.2
	Silica-phenolic carborazole	18	(c)	0.79	3.1	0.51	2.0	0.31	12.2
C	Silica-rubber	16	(c)	3.6	14	2.8	11	0.25	10.0
D	Asbestos-phenolic	9	(c)	1.0	4	5.1	20	0.76	29.8
		10		4.6	18	4.6	18	.92	36.4
	Glass-phenolic	6	(c)	2.5	10	4.6	18	.84	33.0
		8	(c)	4.6	18	6.6	26	.88	34.8
		7	(c)	4.6	18	5.8	23	1.05	41.4
E	Silica-polyurethane	10	(c)	4.6	18	43.2	170	(d)	(d)
	Silica, asbestos-acrylic rubber	17	(c)	14.0	55	7.1	28	3.0	118
	Glass-PVC	14	(c)	5.6	22	16.3	64	4.98	196
	Silica, asbestos-rubber	13	(c)	9.1	36	6.4	25	2.97	117
	Asbestos-PVC	15	(c)	8.9	35	35.6	140	6.60	260

[a]See table I.

[b]Occurs between Mach 0.8 and 1.2.

[c]Not available.

[d]Not applicable.

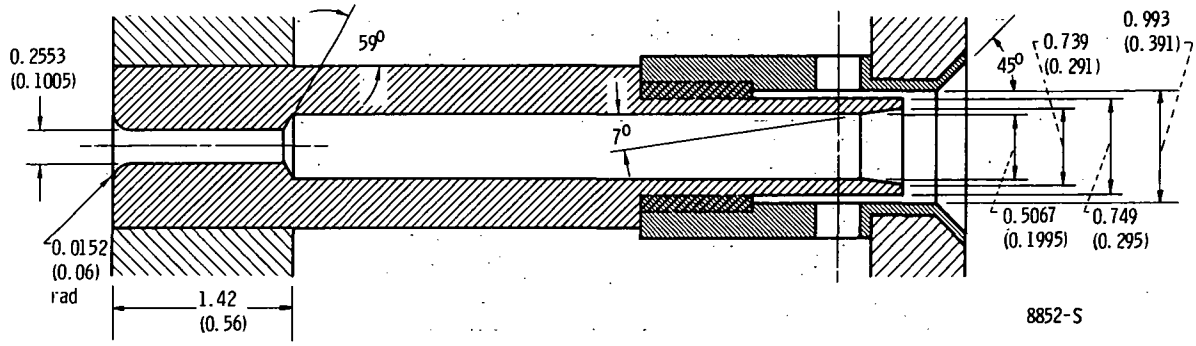

Figure 1. - Detail of injector element. (Dimensions are in cm (in.).)

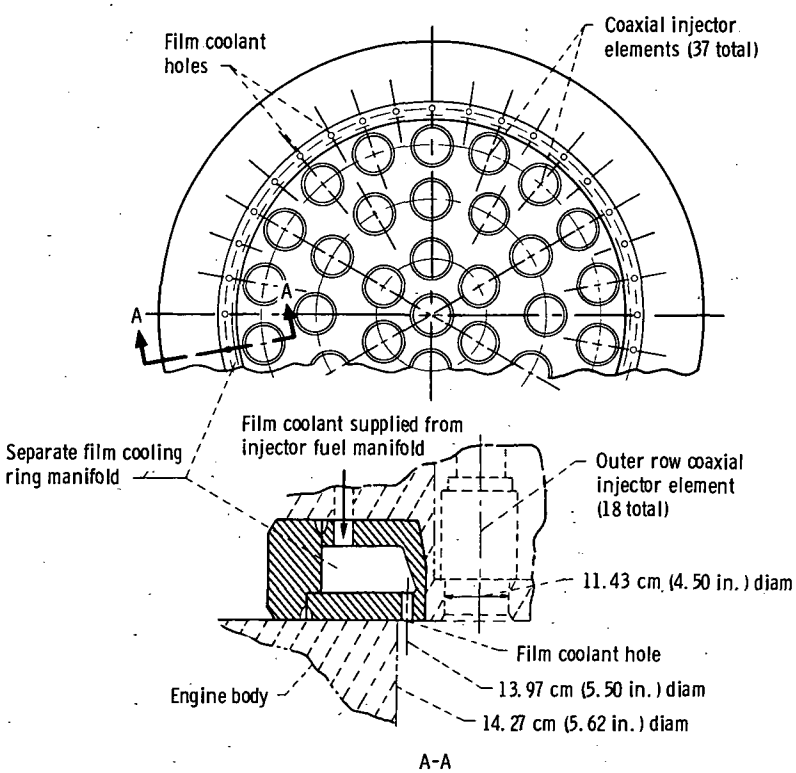

Figure 2. - 37-Element injector with removable film coolant ring manifold.

Configuration	Number of holes	Hole diameter		Cooling area		Hydrogen element area		Total hydrogen area		Ratio of zone area to total area	Nominal percent of fuel film cooling
		cm.	in.	cm^2	in^2	cm^2	in^2	cm^2	in^2		
1A	36	0.165	0.0649	0.768	0.1190	3.35	0.5200	4.123	0.6390	0.186	20
1B	36	.118	.0465	.395	.0612			3.750	.5812	.105	10
2	36	.163	.0640	.748	.1159			4.103	.6359	.182	20
3	54	.135	.0531	.771	.1195			4.103	.6359	.187	
4	18	.236	.0930	.789	.1223			4.144	.6423	.190	
5	36	.118	.0465	.781	.1210			4.135	.6410	.188	
	18	.165	.0650								
6	36	.118	.0465	.395	.0612			3.750	.5812	.105	10

Parallel stream configurations

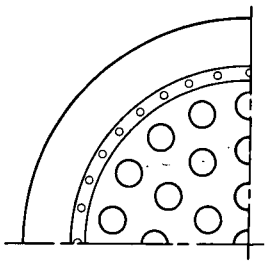

Configuration 1A: 36 equally spaced holes, all parallel to wall; 18 holes are in line with outer-row injection elements and 18 are located midway between two elements.

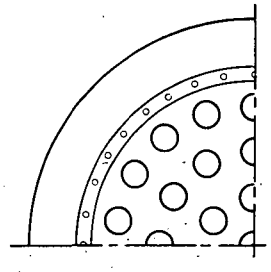

Configuration 1B: Same as 1A except that holes are smaller.

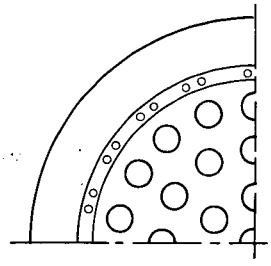

Configuration 2: 18 pairs of holes, parallel to wall. Each pair 0.508 cm (0.2 in.) a part, straddling the center of each outer-row injection element.

Impinging stream configurations

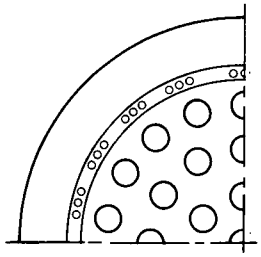

Configuration 3: 18 groups of 3 equal holes, each group impinging on an outer-row injection element stream 3.8 cm (1.5 in.) from injector face.

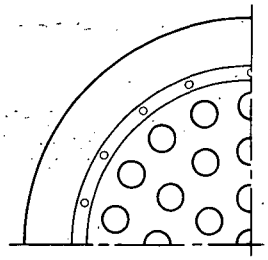

Configuration 4: 18 holes, each impinging on an outer-row injection element stream 3.8 cm (1.5 in.) from injector face.

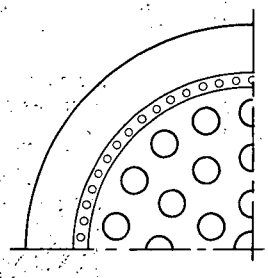

Configuration 5: 18 groups of 3 unequal holes, each group impinging on an outer-row injection element stream; center hole impinges 3.8 cm (1.5 in.), others, 1.3 cm (0.5 in.) from injector face.

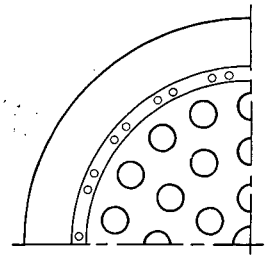

Configuration 6: 18 groups of 2 equal holes impinging on an outer-row injection element stream 1.3 cm (0.5 in.) from injector face.

Figure 3. - Fuel film cooling schemes.

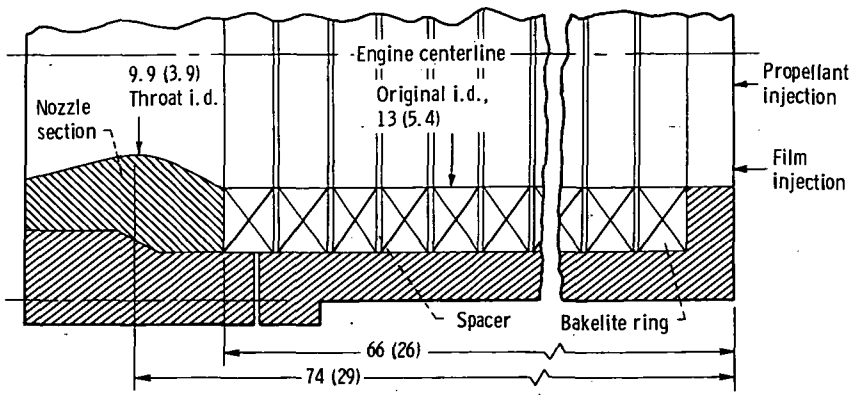

Figure 4. - Chamber assembly using Bakelite indicator rings.
(All linear dimensions are in cm (in.).)

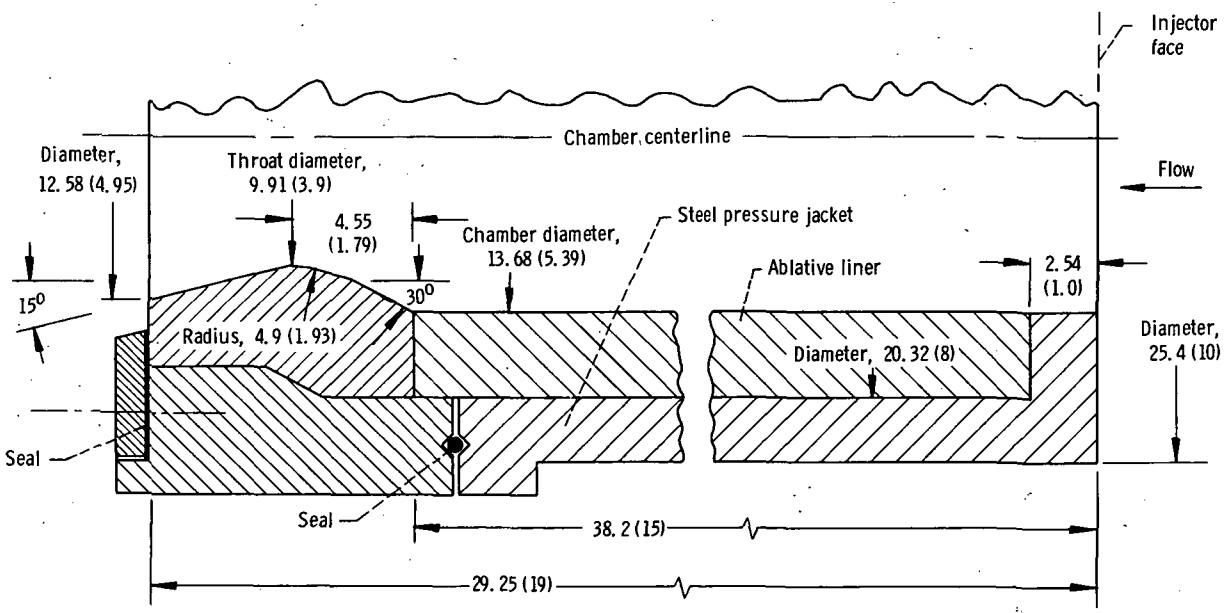

Figure 5. - Heavy wall steel with ablative liner thrust chamber.
(All dimensions in cm (in.) unless indicated otherwise.)

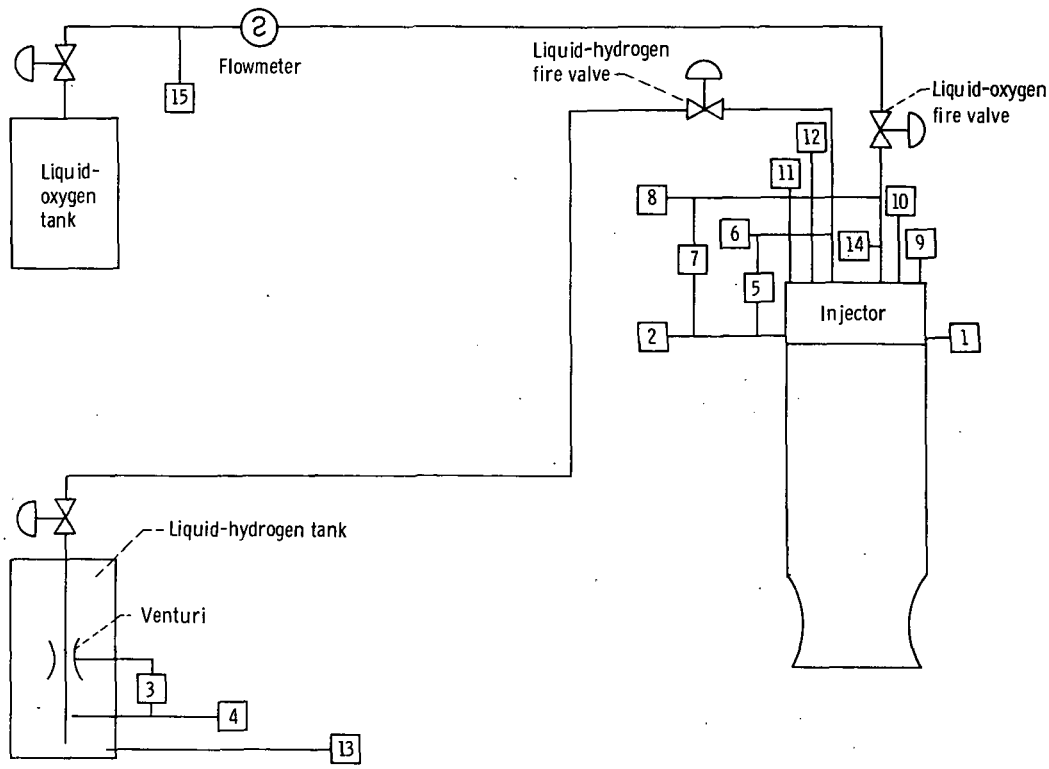

1 Static chamber pressure (injector face), four-arm strain-gage transducer 1
2 Static chamber pressure (injector face), four-arm strain-gage transducer 2
3 Liquid-hydrogen venturi differential pressure, four-arm strain-gage transducer
4 Liquid-hydrogen venturi pressure, four-arm strain-gage transducer
5 Hydrogen-injection differential pressure, four-arm strain-gage transducer
6 Hydrogen-injector pressure, four-arm strain-gage transducer
7 Oxygen-injection differential pressure, four-arm strain-gage transducer
8 Oxygen-injector pressure, four-arm strain-gage transducer
9 Hydrogen-injector temperature, carbon-resistor-sensor probe 1
10 Hydrogen-injector temperature, carbon-resistor-sensor probe 2
11 Hydrogen-injector temperature, carbon-resistor-sensor probe 3
12 Hydrogen-injector temperature, carbon-resistor-sensor probe 4
13 Liquid-hydrogen venturi temperature, platinum resistor sensor
14 Oxygen-injector temperature, copper-constantan thermocouple
15 Oxygen flowmeter temperature, platinum resistor sensor

Figure 6. - Instrumentation diagram.

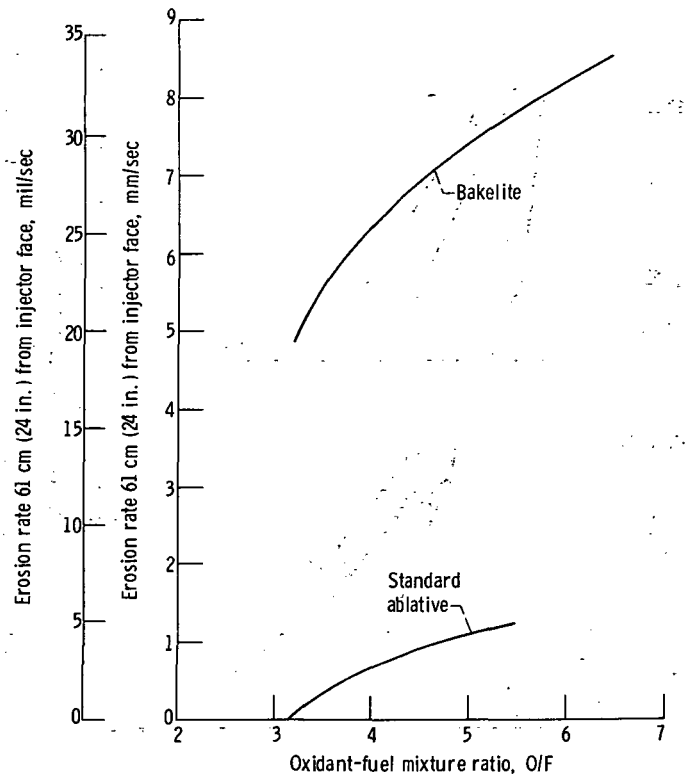

Figure 7. - Comparison of average chamber erosion rates using *Bakelite and standard silica-phenolic ablative as functions of* oxidant-fuel mixture ratio.

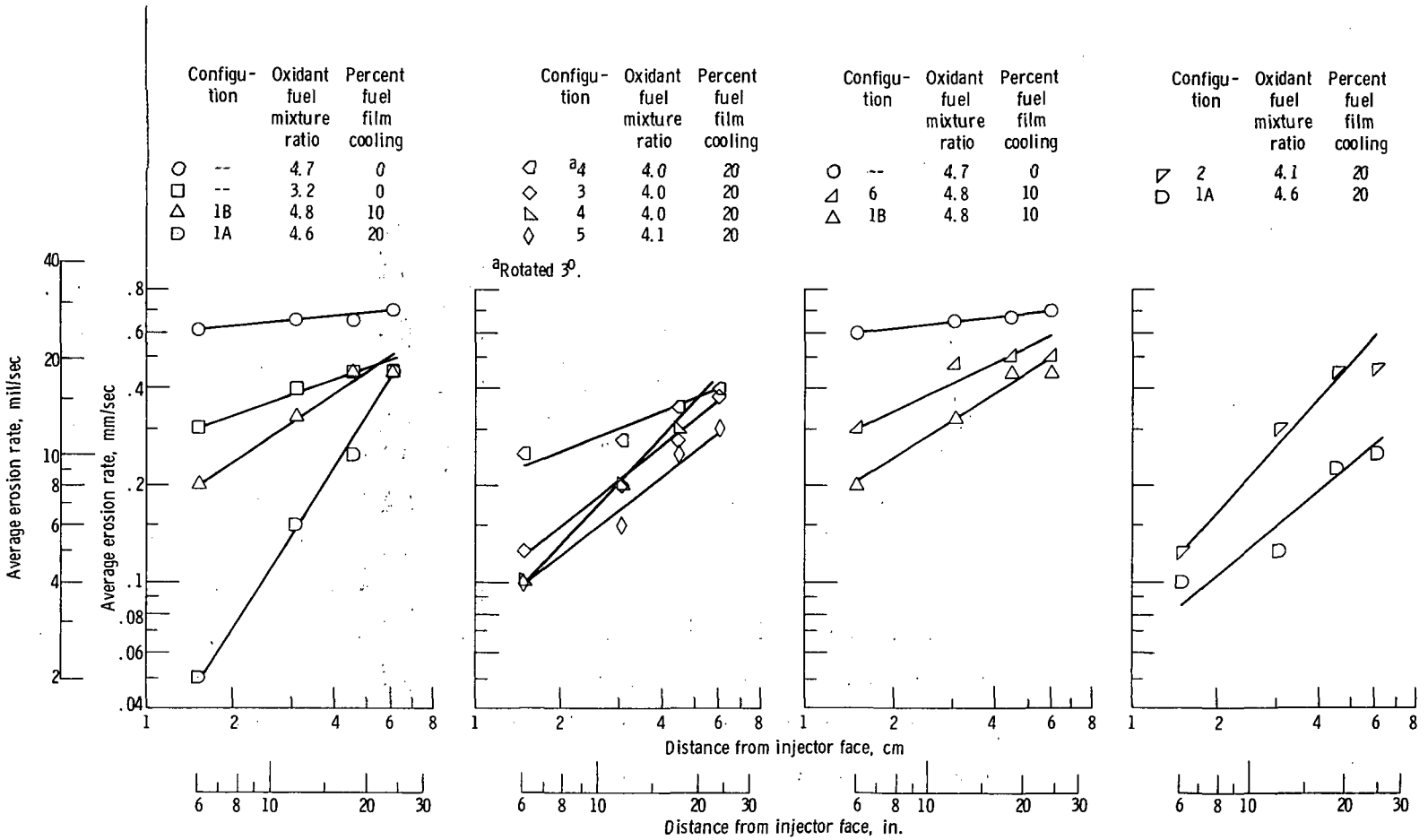

(a) Effect of oxidant-fuel ratio and of fuel film cooling flow rate.

(b) Effect of impinging film coolant streams on outer-row injection element streams.

(c) Comparison of impinging stream, parallel stream, and no stream (no film cooling).

(d) Effect of coolant hole spacing.

Figure 8. - Comparisons of chamber erosion rates with Bakelite indicator material as function of distance from the injector face for each of the film-cooling configurations.

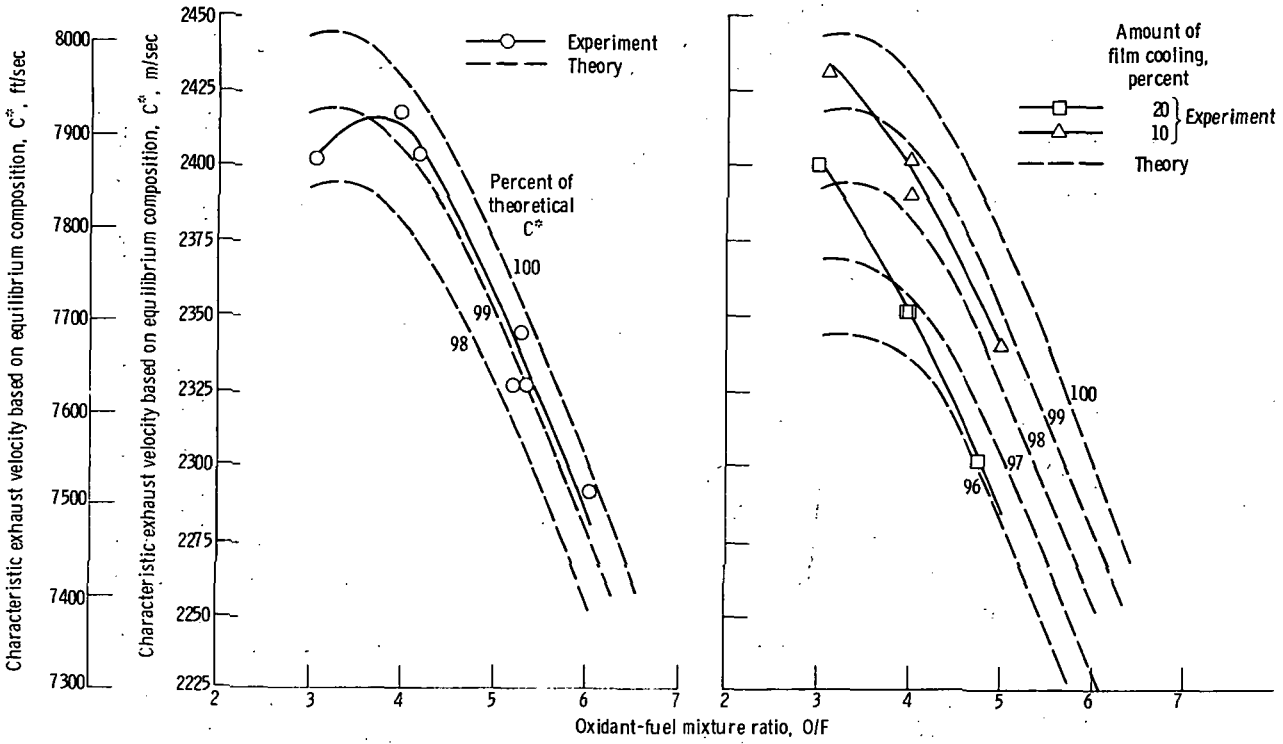

Figure 9. - Comparison of effect of film cooling on characteristic exhaust velocity as function of oxidant-fuel ratio.

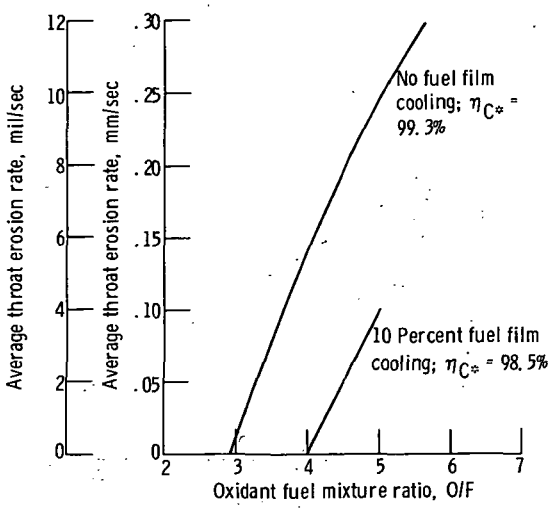

Figure 10. - Comparison of average throat erosion rates with and without film cooling as function of oxidant-fuel mixture ratio.

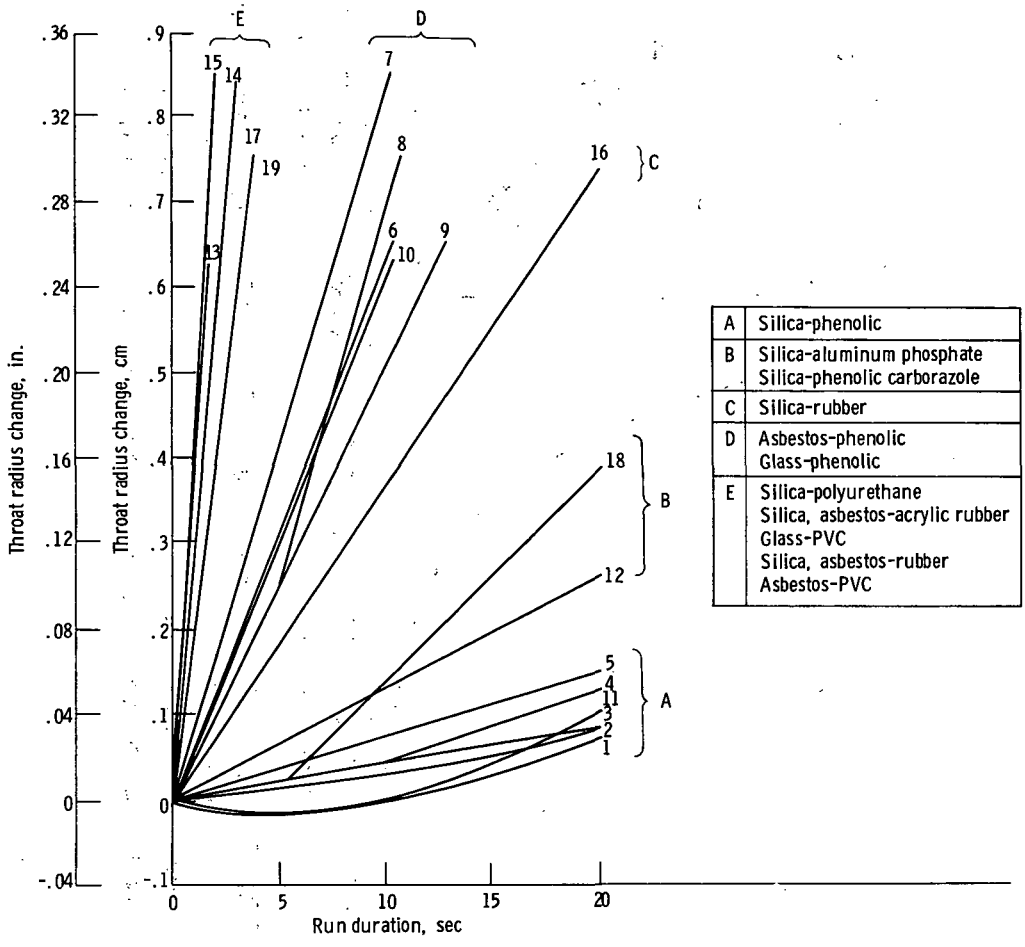

Figure 11. - Throat radius change as function of time for five types of ablative material. Oxidant-fuel mixture ratio, 4.5.

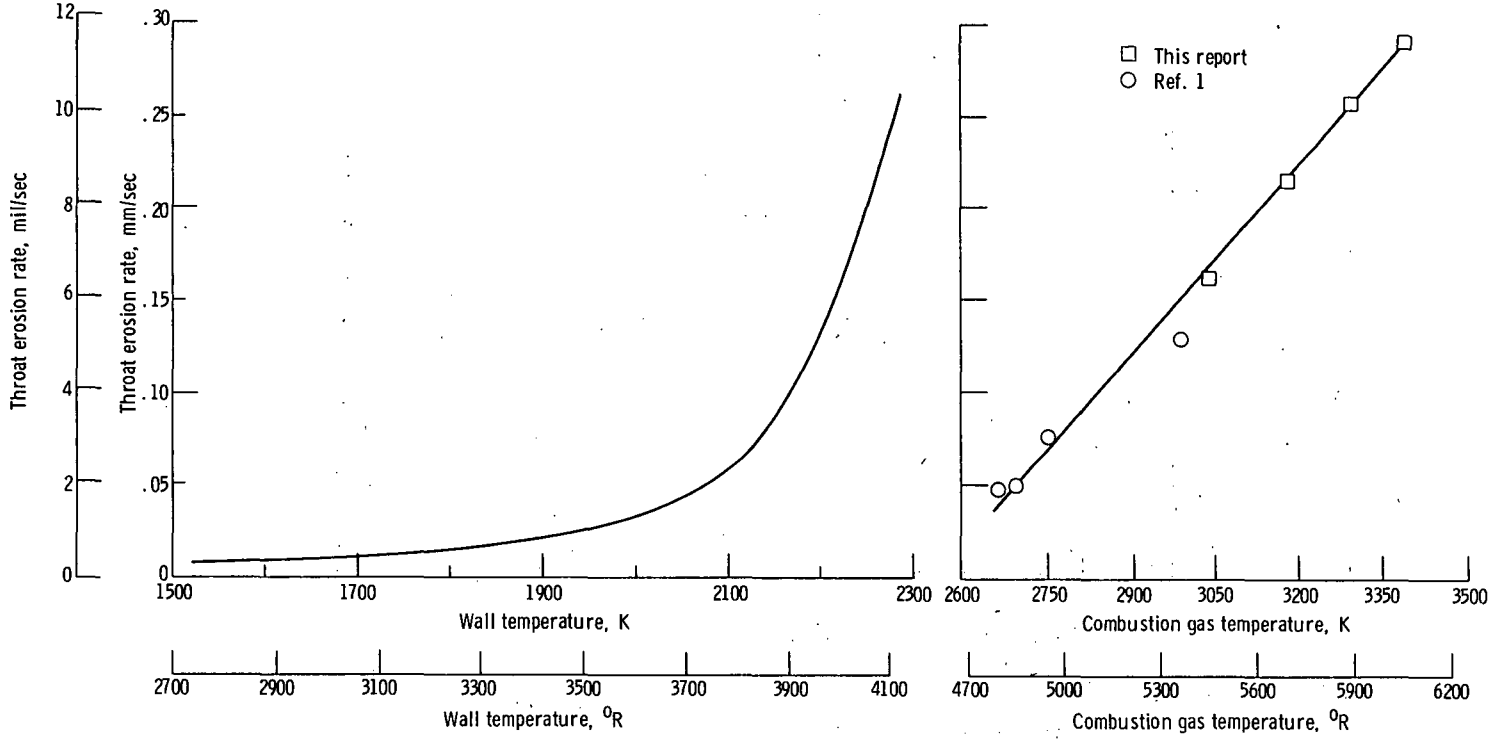

(a) Empirically derived wall temperature (ref. 2).

(b) Combustion gas temperature.

Figure 12. - Average throat erosion rate as function of temperature for silica-phenolic ablative material.

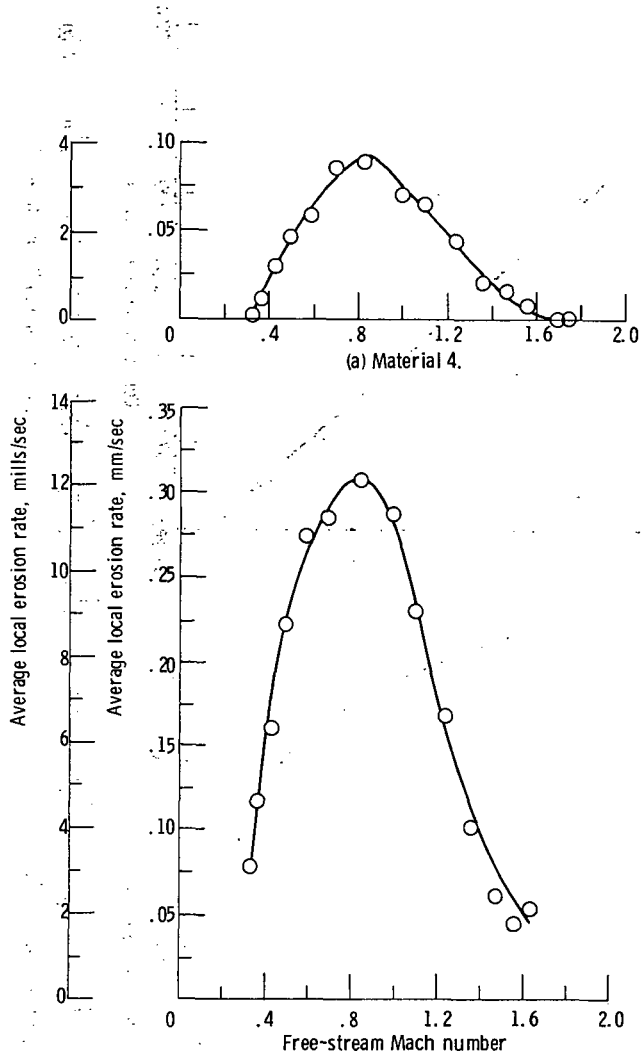

Figure 13. - Average local erosion rate as function of local free-stream Mach number for converging-diverging nozzle section.

1. Report No. NASA TP-1098	2. Government Accession No.	3. Recipient's Catalog No.
4. Title and Subtitle HYDROGEN FILM COOLING OF A SMALL HYDROGEN-OXYGEN THRUST CHAMBER AND ITS EFFECT ON EROSION RATES OF VARIOUS ABLATIVE MATERIALS		5. Report Date December 1977 6. Performing Organization Code
7. Author(s) Ned Hannum, William E. Roberts, and Louis M. Russell		8. Performing Organization Report No. E-8909
9. Performing Organization Name and Address National Aeronautics and Space Administration Lewis Research Center Cleveland, Ohio 44135		10. Work Unit No. 506-21 11. Contract or Grant No.
12. Sponsoring Agency Name and Address National Aeronautics and Space Administration Washington, D.C. 20546		13. Type of Report and Period Covered Technical Paper 14. Sponsoring Agency Code
15. Supplementary Notes		

16. Abstract

An experimental investigation was conducted to determine what arrangement of film-coolant-injection orifices should be used to decrease the erosion rates of small, high-temperature, high-pressure ablative thrust chambers without incurring a large penalty in combustion performance. All of the film cooling was supplied through holes in a ring between the outer row of injector elements and the chamber wall. The best arrangement, which had twice the number of holes as there were outer-row injection elements, was also the simplest. The performance penalties, presented as a reduction in characteristic exhaust velocity efficiency, were 0.8 and 2.8 percentage points for the 10 and 20 percent cooling flows, respectively. The best film-coolant injector was then used to obtain erosion rates for 19 ablative materials. The throat erosion rate was reduced by a factor of 2.5 with a 10-percent coolant flow. Only the more expensive silica-phenolic materials had low enough erosion rates to be considered for use in the nozzle throat. However, some of the cheaper materials might qualify for use in other areas of small nozzles or in nozzles with large throat diameters where the higher erosion rates are more acceptable.

17. Key Words (Suggested by Author(s)) Film cooling Ablative materials Hydrogen-oxygen combustion	18. Distribution Statement Unclassified - unlimited STAR Category 20		
19. Security Classif. (of this report) Unclassified	20. Security Classif. (of this page) Unclassified	21. No. of Pages 26	22. Price* A03

* For sale by the National Technical Information Service, Springfield, Virginia 22161

NASA-Langley, 1977

National Aeronautics and
Space Administration

Washington, D.C.
20546

Official Business
Penalty for Private Use, $300

THIRD-CLASS BULK RATE

Postage and Fees Paid
National Aeronautics and
Space Administration
NASA-451

NASA

POSTMASTER: If Undeliverable (Section 158 Postal Manual) Do Not Return